

# NATIONAL ADVISORY COMMITTEE FOR AERONAUTICS

TECHNICAL NOTE 2307

A THEORETICAL METHOD OF DETERMINING THE CONTROL GEARING  
AND TIME LAG NECESSARY FOR A SPECIFIED DAMPING  
OF AN AIRCRAFT EQUIPPED WITH A  
CONSTANT-TIME-LAG AUTOPILOT

By Ordway B. Gates, Jr., and Albert A. Schy

Langley Aeronautical Laboratory  
Langley Field, Va.



Washington  
March 1951

Reproduced From  
Best Available Copy

20000816 130

1  
NATIONAL ADVISORY COMMITTEE FOR AERONAUTICS

TECHNICAL NOTE 2307

A THEORETICAL METHOD OF DETERMINING THE CONTROL GEARING  
AND TIME LAG NECESSARY FOR A SPECIFIED DAMPING  
OF AN AIRCRAFT EQUIPPED WITH A  
CONSTANT-TIME-LAG AUTOPILOT

By Ordway B. Gates, Jr., and Albert A. Schy

SUMMARY

A method is presented for determining the control gearing and time lag necessary for a specified damping of the motions of an aircraft equipped with an autopilot having constant-time-lag characteristics. The method is applied to a typical present-day airplane equipped with an autopilot which applies rudder control proportional to the yawing angular acceleration. The types of motion predicted for this airplane-autopilot system by this method are in very good agreement with the airplane motions calculated by a step-by-step procedure.

For some values of control gearing there may exist more than one range of time lag for which the motions of the assumed aircraft-autopilot system will have more than a specified amount of damping.

INTRODUCTION

Many present-day aircraft designed to fly at transonic and supersonic speeds have exhibited poor lateral stability characteristics. As a result, much interest has been shown in automatic stabilization systems as a means of obtaining satisfactory stability for high-speed flight. In analyzing the effect of a particular autopilot, the usual practice has been to determine whether the aircraft-autopilot system is stable by employing methods such as those presented in reference 1 (frequency-response analysis) and reference 2 (Nyquist plots). For autopilots characterized by constant time lag (linear variation of control gearing and phase lag with frequency) the same information can be obtained by carrying out an analysis such as that of reference 3. This type of

information is important in the analysis of an autopilot-aircraft system but affords little quantitative indication of the degree of stability which can be obtained by use of a particular autopilot. Since one of the purposes of equipping an aircraft with an autopilot is to improve its stability, the determination of the type of autopilot frequency response that will result in satisfactory stability appears to be of greater importance. The degree of stability which can be obtained by equipping an aircraft with a linear autopilot can be calculated by the methods of reference 4, but, if an over-all picture is desired of the variation of stability for different combinations of control gearing and constant time lag, the calculations become too laborious for practical application. A method of obtaining this information was discussed very briefly in the appendix of reference 4, but has been found inadequate for a comprehensive analysis of autopilot systems which exhibit constant-control-gearing and constant-time-lag characteristics.

The purpose of the present paper, therefore, is to extend the concept discussed in the appendix of reference 4 and thereby present a rigorous method of obtaining the combinations of constant control gearing and constant time lag necessary to provide specified amounts of damping, up to the maximum obtainable, to the motions of a linear oscillating system, with application to the automatic stabilization of aircraft. The method presented is applicable, in a strict sense, only to control systems which exhibit linear frequency-response characteristics, but, under certain conditions discussed in the paper, the analysis is valid for systems having a frequency response similar to that of a constant-time-lag system over a limited range of frequencies.

Although in this paper the method is applied to the problem of automatic stabilization of aircraft, it is, in general, applicable to any linear oscillating system with constant time lag.

#### SYMBOLS AND COEFFICIENTS

$\phi$	angle of roll, radians
$\psi$	angle of yaw, radians
$\beta$	angle of sideslip, radians ( $v/V$ )
$r$	yawing angular velocity, radians per second ( $d\psi/dt$ )
$\ddot{\psi}$	yawing angular acceleration, radians per second per second ( $d^2\psi/dt^2$ )

$p$	rolling angular velocity, radians per second ( $d\phi/dt$ )
$v$	sideslip velocity along lateral axis, feet per second
$V$	airspeed, feet per second
$\rho$	mass density of air, slugs per cubic foot
$q$	dynamic pressure, pounds per square foot $\left(\frac{1}{2}\rho V^2\right)$
$b$	wing span, feet
$S$	wing area, square feet
$W$	weight of airplane, pounds
$m$	mass of airplane, slugs ( $W/g$ ); any integer
$g$	acceleration due to gravity, feet per second per second
$\mu_b$	relative-density factor ( $m/\rho S b$ )
$\eta$	inclination of principal longitudinal axis of airplane with respect to flight path, positive when principal axis is above flight path at nose, degrees
$\gamma$	angle of flight path to horizontal axis, positive in a climb, degrees
$k_{X_0}$	radius of gyration in roll about principal longitudinal axis, feet
$k_{Z_0}$	radius of gyration in yaw about principal vertical axis, feet
$K_{X_0}$	nondimensional radius of gyration in roll about principal longitudinal axis $(k_{X_0}/b)$
$K_{Z_0}$	nondimensional radius of gyration in yaw about principal vertical axis $(k_{Z_0}/b)$
$K_X$	nondimensional radius of gyration in roll about longitudinal stability axis $\left(\sqrt{K_{X_0}^2 \cos^2 \eta + K_{Z_0}^2 \sin^2 \eta}\right)$
$K_Z$	nondimensional radius of gyration in yaw about vertical stability axis $\left(\sqrt{K_{Z_0}^2 \cos^2 \eta + K_{X_0}^2 \sin^2 \eta}\right)$

$K_{XZ}$       nondimensional product-of-inertia parameter  
 $\left( (K_{Z_0}^2 - K_{X_0}^2) \sin \eta \cos \eta \right)$

$C_L$       trim lift coefficient  $\left( \frac{W \cos \gamma}{qS} \right)$

$C_l$       rolling-moment coefficient  $\left( \frac{\text{Rolling moment}}{qSb} \right)$

$C_n$       yawing-moment coefficient  $\left( \frac{\text{Yawing moment}}{qSb} \right)$

$C_Y$       lateral-force coefficient  $\left( \frac{\text{Lateral force}}{qS} \right)$

$$C_{l\beta} = \frac{\partial C_l}{\partial \beta}$$

$$C_{n\beta} = \frac{\partial C_n}{\partial \beta}$$

$$C_{Y\beta} = \frac{\partial C_Y}{\partial \beta}$$

$$C_{nr} = \frac{\partial C_n}{\partial \frac{rb}{2V}}$$

$$C_{np} = \frac{\partial C_n}{\partial \frac{pb}{2V}}$$

$$C_{lp} = \frac{\partial C_l}{\partial \frac{pb}{2V}}$$

$$C_{Yp} = \frac{\partial C_Y}{\partial \frac{pb}{2V}}$$

$$C_{Yr} = \frac{\partial C_Y}{\partial \frac{rb}{2V}}$$

$$C_{l_r} = \frac{\partial C_l}{\partial \frac{rb}{2V}}$$

$$C_{n\delta_r} = \frac{\partial C_n}{\partial \delta_r}$$

$$C_{n\delta_a} = \frac{\partial C_n}{\partial \delta_a}$$

$$C_{l\delta_a} = \frac{\partial C_l}{\partial \delta_a}$$

$$C_{l\delta_r} = \frac{\partial C_l}{\partial \delta_r}$$

$$C_{Y\delta_a} = \frac{\partial C_Y}{\partial \delta_a}$$

$$C_{Y\delta_r} = \frac{\partial C_Y}{\partial \delta_r}$$

t	time, seconds
s <sub>b</sub>	nondimensional time parameter based on span (Vt/b)
D <sub>b</sub>	differential operator $\left(\frac{d}{ds_b}\right)$
P	period of oscillation, seconds
T <sub>1/2</sub>	time for amplitude of oscillation to damp to one-half its original value, seconds
δ <sub>r</sub> , δ <sub>a</sub>	deflection of control surfaces, radians
a	real part of complex root of characteristic stability equation
ω	angular frequency, radians per second
ω <sub>s</sub>	nondimensional angular frequency $\left(\frac{b}{V}\omega\right)$
λ	complex root of characteristic stability equation (a + iω <sub>s</sub> )

- $\tau$  time lag between signal for control and its actual motion, seconds
- $\tau_s$  nondimensional time lag  $\left(\frac{V}{b} \tau\right)$
- $k$  amplitude of control-surface oscillation produced by autopilot in response to oscillation of airplane acceleration  $\left(\left|\frac{\delta_r}{\ddot{\psi}}\right|_{\text{autopilot}}\right)$
- $k_s = \left|\frac{\delta_r}{D_b^2 \psi}\right| = \frac{V^2}{b^2} k$
- $\theta$  phase angle, radians

## EQUATIONS OF MOTION

The nondimensional linearized equations of motion, referred to the stability axes, are:

Yawing

$$2\mu_b(K_Z^2 D_b^2 \psi + K_{XZ} D_b^2 \phi) = C_{n\beta} \beta + \frac{1}{2} C_{n\dot{\beta}} D_b \phi + \frac{1}{2} C_{n\dot{r}} D_b \psi + C_{n\delta_r} \delta_r \quad (1a)$$

Rolling

$$2\mu_b(K_X^2 D_b^2 \phi + K_{XZ} D_b^2 \psi) = C_{l\beta} \beta + \frac{1}{2} C_{l\dot{\beta}} D_b \phi + \frac{1}{2} C_{l\dot{r}} D_b \psi + C_{l\delta_a} \delta_a \quad (1b)$$

Sideslipping

$$2\mu_b(D_b \beta + D_b \psi) = C_{Y\beta} \beta + \frac{1}{2} C_{Y\dot{\beta}} D_b \phi + C_{L\dot{\phi}} \phi + \frac{1}{2} C_{Y\dot{r}} D_b \psi + (C_L \tan \gamma) \psi \quad (1c)$$

The derivatives  $C_{n\delta_a}$ ,  $C_{l\delta_r}$ ,  $C_{Y\delta_a}$ , and  $C_{Y\delta_r}$  have been neglected in equations (1).

If a constant-time-lag autopilot which applies rudder control proportional to the  $n$ th derivative of the yawing displacement is installed in the airplane, the equation for  $\delta_r$  as a function of  $s_b$  becomes

$$\delta_r(s_b) = \frac{\partial \delta_r}{\partial D_b^n \psi} D_b^n \psi(s_b - \tau_s) \quad (2)$$

where the term  $D_b^n \psi(s_b - \tau_s)$  signifies that the control deflection at a given instant is proportional to the nth derivative of  $\psi$  which existed at a fixed time  $\tau_s$  previous to the given instant. The term  $\frac{\partial \delta_r}{\partial D_b^n \psi}$  is the control-gearing ratio of the autopilot. Similarly, if a constant-time-lag autopilot which applies aileron control proportional to the nth derivative of the rolling displacement is installed in the airplane, the equation for  $\delta_a$  as a function of  $s_b$  becomes

$$\delta_a(s_b) = \frac{\partial \delta_a}{\partial D_b^n \phi} D_b^n \phi(s_b - \tau_s) \quad (3)$$

For purposes of illustration, assume that the type of autopilot described by equation (2) is to be investigated. Therefore, the value of  $\delta_r$  given by equation (2) is substituted for  $\delta_r$  in equations (1). The aileron deflection  $\delta_a$  is assumed zero. When  $\phi_{oe}^{\lambda s_b}$  is substituted for  $\phi$ ,  $\psi_{oe}^{\lambda s_b}$  for  $\psi$ , and  $\beta_{oe}^{\lambda s_b}$  for  $\beta$  in the resultant equations written in determinant form,  $\lambda$  must be a root of the characteristic stability equation

$$A\lambda^5 + B\lambda^4 + C\lambda^3 + D\lambda^2 + E\lambda + k_s \lambda^n e^{-\tau_s \lambda} (A'\lambda^3 + B'\lambda^2 + C'\lambda + D') = 0 \quad (4)$$

where  $A$ ,  $B$ ,  $C$ ,  $D$ ,  $E$ ,  $A'$ ,  $B'$ ,  $C'$ , and  $D'$  are functions of the mass and aerodynamic parameters of the airplane. The expressions for  $A$ ,  $B$ ,  $C$ ,  $D$ , and  $E$  are given in reference 5, and, for this particular case,

$$A' = -I_{\mu_b}^2 K_X^2 C_{n\delta_r}$$

$$B' = (2\mu_b K_X^2 C_{Y\beta} + \mu_b C_{l_p}) C_{n\delta_r}$$

$$C' = \left( -\frac{1}{2} C_{l_p} C_{Y\beta} + \frac{1}{2} C_{Y_p} C_{l_\beta} \right) C_{n\delta_r}$$

$$D' = C_L C_{l_\beta} C_{n\delta_r}$$

$$\text{and } k_s = \frac{\partial \delta_r}{\partial D_b^n \psi}$$



The time to damp and the period of the lateral oscillation in seconds are given by the expressions

$$\left. \begin{aligned} T_{1/2} &= \frac{-0.693}{a} \frac{b}{V} \\ P &= \frac{2\pi}{\omega_s} \frac{b}{V} \end{aligned} \right\} \quad (5)$$

where  $a$  and  $\omega_s$  are the real and imaginary parts, respectively, of a complex root of equation (4).

### ANALYSIS

The following assumptions are made in the derivation of the method which may be used to determine the combinations of  $k_s$  and  $\tau_s$  necessary to provide a specified amount of damping of the lateral oscillations of an automatically stabilized airplane:

(1) The characteristic stability equation of an airplane equipped with an autopilot which applies rudder control proportional to the  $n$ th derivative of the yawing displacement which existed at time  $s_p - \tau_s$  is given by equation (4); that is, the autopilot is assumed to have linear characteristics.

(2) This stability equation has as one of its roots  $\lambda = a + i\omega_s$ . (This root  $\lambda$  represents an oscillatory mode of motion, the time to damp to one-half amplitude and the period of which are given by equations (5).)

The stability equation of the airplane-autopilot system (equation (4)) may be rewritten in the following form:

$$k_s e^{-\tau_s \lambda} = \frac{A\lambda^5 + B\lambda^4 + C\lambda^3 + D\lambda^2 + E\lambda}{-\lambda^n (A'\lambda^3 + B'\lambda^2 + C'\lambda + D')} \quad (6)$$

If  $\lambda = a + i\omega_s$  is substituted in each side of equation (6), the condition that  $\lambda$  be a root of the characteristic stability equation is that the complex number  $A_1 + iB_1$  obtained from the left-hand side must be equal to the one obtained from the right-hand side  $A_2 + iB_2$ . The quantities  $A_1 + iB_1$  and  $A_2 + iB_2$  may be represented by the expressions  $R_1 e^{i\theta_1}$  and  $R_2 e^{i\theta_2}$ , respectively. Therefore, this requirement is equivalent to saying that  $R_1 = R_2$  and  $\theta_1 = \theta_2$  if  $\lambda$  is to be a

root of equation (4). If  $\lambda = a + i\omega_s$  is substituted in the left-hand side of equation (6), the following expression results:

$$k_s e^{-\tau_s a} \left( \cos \tau_s \omega_s - i \sin \tau_s \omega_s \right) \equiv A_1 + iB_1 \equiv R_1 e^{i\theta_1}$$

Since the complex number  $A_1 + iB_1$  is unchanged when its phase angle is increased by integral multiples of  $2\pi$ , the following identities exist:

$$R_1 \equiv (k_s)_m e^{-(\tau_s)_m a}$$

$$\theta_1 \equiv 2\pi m - (\tau_s)_m \omega_s$$

where  $m = 0, 1, 2, \dots$ . If  $\lambda = a + i\omega_s$  is substituted in the right-hand side of equation (6), the values of  $R_2$  and  $\theta_2$  can be calculated numerically. For each value of  $m$ , the value of  $(\tau_s)_m$  necessary to make  $\theta_1$  equal to  $\theta_2$  can be calculated and since  $a$  is a known fixed quantity, the values of  $(k_s)_m$  necessary to make  $R_1$  equal to  $R_2$  can also be determined. For the combinations  $(\tau_s)_1$  and  $(k_s)_1$ ,  $(\tau_s)_2$  and  $(k_s)_2$ ,  $\dots$ ,  $(\tau_s)_m$  and  $(k_s)_m$ , therefore,  $\lambda = a + i\omega_s$  is a root of the characteristic stability equation (equation (4)). The parameter  $m$  in the preceding equations is necessary if the analysis is to hold for values of  $a$  which represent dampings less than the natural airplane damping. More specifically, the ranges of  $\tau_s$  and  $k_s$  which result in greater stability than the natural stability of the airplane alone cannot be obtained correctly by utilizing the methods as presented in reference 4. For example, the curves presented in figure 10 of reference 4 fail to provide the important information that, for small values of  $\tau_s$ , the autopilot-airplane system discussed in that reference is less stable than the airplane alone. In addition, the parameter  $m$  is necessary if the analysis is to hold for values of  $\tau_s > \frac{2\pi}{\omega_s}$ . These values of  $\tau_s$  must be included in a theoretical analysis of the problem since, as  $\tau_s$  is increased by multiples of  $\frac{2\pi}{\omega_s}$ , the phase relation again exists which is necessary for the system to have an oscillatory mode the damping of which is indicated by  $a$ . The analysis of reference 4 considered only the case of  $m = 1$  and was therefore restricted to values of  $\tau_s < \frac{2\pi}{\omega_s}$  or, in effect, to values less than the natural period of the oscillation.

For a given value of  $a$  corresponding to some desired value of  $T_{1/2}$  of the lateral oscillation, the analysis may be made throughout the range of  $\omega_s$  and the required combinations of  $(k_s)_m$  and  $(\tau_s)_m$  determined for each  $\omega_s$ . For each  $m$ , therefore, a curve representing this value of  $a$  may then be plotted as a function of  $(k_s)_m$  and  $(\tau_s)_m$ . This family of  $m$  curves will divide the  $k_s, \tau_s$  plane into regions for which the lateral oscillations will have more or less damping than that indicated by the value of  $a$  being investigated.

General expressions for  $(\tau_s)_m$  and  $(k_s)_m$  for each  $\omega_s$ , in terms of  $R_2$  and  $\theta_2$ , are as follows:

$$(\tau_s)_m = (\tau_s)_0 + \frac{2\pi m}{\omega_s}$$

$$(k_s)_m = (k_s)_0 e^{2\pi m a / \omega_s}$$

where

$$(\tau_s)_0 = -\frac{\theta_2}{\omega_s}$$

$$(k_s)_0 = R_2 e^{(\tau_s)_0 a} = R_2 e^{-\theta_2 a / \omega_s}$$

Thus, for any value of  $\omega_s$ , it is necessary only to obtain  $(\tau_s)_0$  and  $(k_s)_0$  since, by use of the preceding generating functions, the required combination of  $\tau_s$  and  $k_s$  are readily obtained for any integral value of  $m$ .

#### ILLUSTRATIVE EXAMPLES AND DISCUSSION

Since the purpose of installing an autopilot is to improve the lateral stability of the airplane, one logical value of  $a$  to investigate would be that value which corresponds to the damping of the lateral oscillation of the airplane without the autopilot installed, hereinafter referred to as airplane damping. Thus, the curves corresponding to that value of  $a$  would indicate those combinations of  $k_s$  and  $\tau_s$  for which the airplane is more stable with a given autopilot than without it. This value of  $a$  may be determined, of course, by solving for the complex roots of the characteristic stability equation when  $k_s$  is set equal to zero. The family of curves obtained for this value of  $a$  forms the boundary between two different types of curves; that is, the curves for

dampings greater than the airplane damping are of a different shape than those for dampings less than this value. This change in the damping curves is discussed in detail in a subsequent paragraph.

For purposes of illustrating the present method, the airplane is assumed to have freedom only in yaw. Several damping curves were calculated for a typical present-day airplane equipped with an autopilot sensitive to yawing acceleration for both the three-degree-of-freedom and the one-degree-of-freedom cases. The results of the calculations, although not always in quantitative agreement, indicated that the nature of the damping curves obtained for both cases was essentially the same and therefore subsequent discussion is based on the results obtained when the system was assumed to have freedom only in yaw.

The mass and aerodynamic characteristics of the typical present-day airplane are presented in table I. The characteristic stability equation for the three-degree-of-freedom case was presented previously (equation (4)), and the characteristic stability equation for the one-degree-of-freedom case is given by

$$2\mu_b K_Z^2 \lambda^2 - \frac{1}{2} C_{n_r} \lambda - C_{n_\psi} = C_{n_{\delta_r}} k_s e^{-\tau_s \lambda} \lambda^2 \quad (7)$$

The derivative  $C_{n_\psi}$  is assumed equal to  $-C_{n_\beta}$ . The equation used in the calculations, obtained by rearranging equation (7), is

$$k_s e^{-\tau_s \lambda} = \frac{2\mu_b K_Z^2 \lambda^2 - \frac{1}{2} C_{n_r} \lambda - C_{n_\psi}}{C_{n_{\delta_r}} \lambda^2} \quad (8)$$

As was pointed out in a previous section, the damping curve corresponding to the damping of the airplane oscillatory motion without the autopilot installed forms the boundary between two characteristically different types of curves. In order to illustrate the types of curves which will be encountered, calculations were made for the airplane damping and for dampings less than and greater than this damping. The results are shown in figure 1. For the airplane described in table I, the airplane damping is  $T_{1/2} = 2.02$  seconds. The values of  $\tau_s$  and  $k_s$  obtained from equation (8) have been converted from the nondimensional time parameter  $s_b$  to time in seconds. Thus, the curves are plotted as a function of the dimensional parameters  $k$  and  $\tau$  in seconds. Each point on these curves corresponds to a different frequency  $\omega_s$ , which varies from infinity at the point ( $\tau=0, k=0.0628$ ) to zero as  $\tau$  and  $k$  approach infinity. It is interesting to note that all the damping curves approach the point ( $0, 0.0628$ ) as  $\omega_s \rightarrow \infty$ . For this point, the roots of the characteristic stability equation do not indicate any high-frequency oscillation; however, for any finite value of  $\tau$ , the roots of

this equation will indicate a high-frequency oscillation in addition to the usual lateral oscillation. For a given value of  $k$ , the frequency of this additional oscillation decreases with increases in  $\tau$ . Also, all the damping curves approach a minimum value of  $k$  for a value of  $\omega_s$  corresponding to a frequency close to the natural frequency of the airplane. In general, frequencies greater than and less than the airplane natural frequency are separated by the point of minimum  $k$  on each of the damping curves. For this airplane the natural frequency is approximately 5 radians per second.

The curves presented in figure 1(a) correspond to  $T_{1/2} = \infty$ . The complete boundary for neutral stability is made up of the curves for  $m = 0, 1, 2, \dots, \infty$ . Unless  $m$  is allowed to take on integral values it is impossible to define correctly the stable region of the  $k, \tau$  plane. For example, consider the point ( $k=0.035, \tau=1.6$ ) in figure 1(a). The point, according to the curve for  $m = 1$ , represents a stable condition, but since it falls on the unstable side of the  $m = 2$  curve, the presence of unstable oscillatory modes in addition to the stable oscillation is indicated and thus this combination of  $k$  and  $\tau$  would result in an unstable condition. The true boundary of neutral stability is shown as the solid curve of figure 1(a). Only the curves for  $m = 1, 2$ , and  $3$  are shown. The curve for  $m = 0$  would fall in the region corresponding to negative values of  $\tau$  and therefore was omitted. From this figure it is apparent that for some values of  $k$  there exist several ranges of  $\tau$  for which the system will be stable. The width of these ranges diminishes as  $m$  increases and eventually disappears completely. For this special case of  $T_{1/2} = \infty$  and a given value of  $k$ , the ranges of  $\tau$  necessary for stability can be calculated analytically by the methods of reference 3, since the airplane was originally stable. The results obtained by using this method agree exactly with those of figure 1(a). The analysis presented in this reference was for a one-degree-of-freedom system and in appendix A it has been modified to apply to an airplane-autopilot system with three degrees of freedom. It should be emphasized that the method of reference 3 is applicable only to the special case for  $T_{1/2} = \infty$  and an originally stable airplane. On the other hand the method presented in this paper is equally applicable to originally unstable airplanes, in which cases the  $T_{1/2} = \infty$  curves will have the form of the curves for dampings greater than the original airplane damping.

For  $T_{1/2} = 3.50$  seconds, the resulting curves for  $m = 0, 1, 2$ , and  $3$  are presented in figure 1(b). The general shape of the curves is the same as for those of figure 1(a), and the same general conclusions apply. Only that part of the curve for  $m = 0$  which is in the region of positive time lags is shown in the figure. The curves for the airplane damping,  $T_{1/2} = 2.02$  seconds, are shown in figure 1(c). For the

combinations of  $k$  and  $\tau$  within the triangular-like regions, which are formed by the curves for  $m$ ,  $m + 1$ , and  $k = 0$ , the oscillatory motion of the airplane is more stable with the autopilot than without it. The damping curves for  $T_{1/2} = 1.40$  seconds and  $T_{1/2} = 0.70$  second are presented in figures 1(d) and 1(e), respectively, for  $m = 1, 2$ , and 3. These curves are quite different from the ones presented for damping less than the airplane damping. The combinations of  $k$  and  $\tau$  for which the airplane would be more stable than is indicated by the curves for  $T_{1/2} = 1.40$  seconds or  $T_{1/2} = 0.70$  second, for example, are enclosed in island-like regions in the stable part of the  $k, \tau$  plane. A similar region exists for each value of  $m$ , but as  $m$  is increased the size of the region diminishes. In addition, as  $T_{1/2}$  is decreased these looped regions become increasingly smaller for each value of  $m$ . As  $T_{1/2}$  is reduced beyond some finite value these loops will cease to exist. The value of  $T_{1/2}$  for which the  $m = 1$  loop disappears represents the maximum damping obtainable for this airplane by the use of a specific autopilot. A method of obtaining this maximum damping for each value of  $m$  is presented in appendix B. It can be seen from figure 1(e) that no loops exist for  $m > 1$ . This amount of damping, therefore, can only be obtained for all the oscillatory modes within the  $m = 1$  loop. This conclusion could have been reached by carrying out the analysis of appendix B. As a matter of interest, for this particular autopilot-airplane system, the  $m = 1$  loop ceases to exist for  $T_{1/2} < 0.35$  second.

The regions in the  $k, \tau$  plane, which correspond to the dampings shown in figure 1, have been combined and are presented in figure 2. This figure gives an over-all picture of the effects of the specific autopilot on the lateral stability of the airplane. In order to verify the results indicated by this figure, airplane motions were calculated for the combinations of  $k$  and  $\tau$  identified as points A, B, C, and D. Step-by-step calculations were made by assuming freedom only in yaw, and the airplane motions in yaw subsequent to a  $5^\circ$  displacement in yaw for these combinations of  $k$  and  $\tau$  are presented in figure 3. Point A is located within the  $m = 1$  loop corresponding to  $T_{1/2} \leq 1.40$  seconds and the motion of figure 3(a) checks this prediction. The motion for point B (fig. 3(b)) is very lightly damped as is indicated by its nearness to the zero-damping curve. Point C represents a combination of  $k$  and  $\tau$  for which the airplane is less stable with this autopilot than without it. Also, as seen from figure 2, the motion for this combination of  $k$  and  $\tau$  should indicate two oscillatory modes of different frequency with approximately the same amount of damping. The motions of figure 3(c) support this prediction since more than one oscillatory mode is indicated. The combination of  $k$  and  $\tau$  for point D is located within the  $m = 2$  loop,  $T_{1/2} \leq 1.40$  seconds. The motion for this combination (fig. 3(d)) is approximately as heavily damped as that of

figure 3(a), but because of the larger value of time lag this high damping is not realized as quickly. It is of significance, however, that this amount of damping can be obtained for the combinations of  $k$  and  $\tau$  within the  $m = 2, 3, \dots$  loops as well as for those within the  $m = 1$  loop. In actual practice the phase lags encountered in conventional autopilots which can be represented by second-order systems generally do not exceed  $180^\circ$  at any frequency and the assumption of constant-time-lag characteristics usually is valid only within the frequency range where the autopilot phase lag is less than approximately  $90^\circ$ . The time lags common to the  $m = 2, 3, \dots$  loops imply phase shifts greater than  $2\pi$  and thus are beyond the range where the assumption of constant time lag is usually valid. Two conceivable cases may be mentioned for which it might be desirable to develop devices with such large time lags. One is the case of a high-natural-frequency system (not necessarily an aerodynamic system), for which it might be impractical to obtain the small lags necessary for the stability of the system with automatic stabilization in the  $m = 1$  region. Another case is that of an aerodynamic system which is to respond to automatic control in addition to being automatically stabilized, in which case it might be desirable to delay the operation of the stabilization device in order to reduce its effect on the response time of the automatic control.

It should be reemphasized that the preceding analysis was made for an airplane equipped with an autopilot having constant time lag. Damping curves such as those presented in figure 2 therefore apply, in a strict sense, only to autopilots which have these assumed characteristics. If, however, a frequency-response analysis of a given autopilot indicates that the assumption of a constant time lag is valid for only a limited range of frequencies, the preceding methods can still be used to good advantage. Damping curves such as those of figure 2 can be constructed and the values of  $k$  and  $\tau$ , which will result in a given amount of damping of the oscillatory modes of motion, can be determined since for each point in the  $k, \tau$  plane there will be certain complex solutions of the airplane-autopilot characteristic stability equation (equation (7)). If the frequencies of the oscillatory modes characteristic of a particular point in the  $k, \tau$  plane are such that the autopilot can be made to exhibit constant-lag characteristics up to and beyond the highest frequency involved, then the damping of the oscillatory motions for the airplane-autopilot system will be essentially the same as predicted by the constant-time-lag analysis. The validity of this statement can be seen by examination of equation (8). The left-hand side of this equation is the autopilot frequency-response function  $\delta_r/D_b^2\psi$ . Likewise the right-hand side of the equation is the airplane frequency-response function  $\delta_r/D_b^2\psi$ . The necessary and sufficient condition that  $\lambda = a + i\omega_s$  be a solution of the characteristic equation (equation (7)) is that, when  $a + i\omega_s$  is substituted for  $\lambda$  in equation (8), the complex number obtained from the autopilot frequency-response function  $\delta_r/D_b^2\psi$  be

identical with that obtained from the airplane frequency-response function  $\delta_r/D_b^2\psi$ . The frequencies characteristic of any point in the  $k, \tau$  plane are readily identifiable and, if the frequency-response function  $\delta_r/D_b^2\psi$  of an actual autopilot can be closely approximated by the ex-

pression  $\frac{\delta_r}{D_b^2\psi} = k_s e^{-\tau s^\lambda}$  up to and beyond those frequencies, then the

complex roots of the airplane-autopilot characteristic equation must be essentially the same as those predicted by a constant-time-lag analysis.

#### CONCLUDING REMARKS

A method is presented for determining the control gearing and time lag necessary for a specified damping of an aircraft equipped with a constant-time-lag autopilot. The method is applied to a typical present-day airplane equipped with an autopilot which applies rudder control proportional to the yawing angular acceleration. The results calculated for an airplane-autopilot system by the method described are in excellent agreement with the airplane motions calculated by a step-by-step procedure.

The investigation shows that, for some values of control gearing, there exists more than one range of time lag for which the assumed aircraft-autopilot system will have a specified amount of damping. The width of these ranges diminishes with increased time lags, and beyond some value of lag, these ranges cease to exist.

It should be emphasized that the analysis presented in this paper is applicable, in a strict sense, only to systems which exhibit constant-time-lag characteristics; however, under certain conditions discussed in the paper, a constant-time-lag type of analysis is valid for systems which have constant time lags for only a limited range of frequencies.

Langley Aeronautical Laboratory  
National Advisory Committee for Aeronautics  
Langley Field, Va. , September 26, 1950



## APPENDIX A

## EXTENSION OF ANSOFF'S STABILITY CRITERION TO THE LATERAL

## MOTIONS OF AN AIRPLANE EQUIPPED WITH YAW AUTOPILOTS

Reference 3 analyzes the effects of constant time lag in the feedback of a one-degree-of-freedom oscillatory system on the stability of the oscillation. The analysis shows that, in general, for a given gearing, ranges of time lag will exist for which the system remains stable. These ranges are separated from each other by unstable ranges. The expression for these stable time-lag ranges is obtained in closed form in terms of the other parameters of the system. It should be emphasized that the analysis is valid only for a system originally stable without feedback.

This appendix extends the method of reference 3 to the three degrees of freedom of lateral motion of an airplane with a yaw autopilot. The argument and analysis presented in reference 3 are repeated herein only to the extent necessary to present the modifications of the method and to emphasize or clarify points.

The autopilot is assumed to provide a yawing moment proportional to the yaw displacement or to the  $n$ th time derivative of the yaw, with the moment lagging the disturbance by a constant time  $\tau$ . The resulting nondimensional equations of motion are given by equations (1) and (2), and the characteristic stability equation of the system is equation (4). Note that the first five terms of equation (4) are the characteristic function of the airplane without the autopilot installed. If, therefore, equation (4) is divided through by this characteristic function of the airplane alone, the characteristic equation of the total system is obtained in the form

$$F(\lambda) = 1 + \frac{(A'\lambda^3 + B'\lambda^2 + C'\lambda + D')\lambda^{n_k}e^{-\tau_s\lambda}}{A\lambda^5 + B\lambda^4 + C\lambda^3 + D\lambda^2 + E\lambda} \equiv 1 + W(\lambda) = 0 \quad (A1)$$

The theory may be given very briefly as follows: The roots of equation (4) are also the roots of equation (A1) and are the characteristic roots of the system. In order for the system to be stable, their real parts must all be negative. In the complex  $\lambda$ -plane a closed curve consisting of the imaginary axis and the infinite semicircle to its right will enclose all values of  $\lambda$  with positive real parts. Then by a theorem in the theory of functions of a complex variable (see reference 6), it can be shown that the transformation of this closed curve

into the complex F-plane will circle the origin in the F-plane once in a positive direction for each root of  $F(\lambda) = 0$  enclosed by the curve in the  $\lambda$ -plane and once in the negative direction for each pole. It can be seen from equation (A1) that the origin of the F-plane corresponds to the point  $(-1, 0i)$  in the W-plane, and, in fact, each curve in the F-plane is simply displaced unit distance to the left in the W-plane. If the airplane were originally stable,  $F(\lambda)$  would have no poles in the right half of the  $\lambda$ -plane; therefore, the condition that the whole system have no roots in this right half of the plane (unstable roots) is simply that  $W(\lambda)$  should not enclose the  $(-1, 0i)$  point in the W-plane.

One condition for the preceding theorem to apply is that there be no zeros or poles of  $F(\lambda)$  on the boundary curve in the  $\lambda$ -plane. It will be shown subsequently that for  $n > 2$  stability is impossible; thus, the only autopilots of interest are those where  $n = 0, 1$ , and  $2$ , that is, displacement, velocity, or acceleration autopilots. Now the zero root of the characteristic equation (4) for  $n = 1$  and  $2$  is removed by the division which gives equation (A1); therefore, no difficulty occurs for these two cases. For  $n = 0$ , however, equation (A1) gives a pole for  $F(\lambda)$  at  $\lambda = 0$ , which is on the boundary curve; therefore, for  $n = 0$  dividing through by  $\lambda$  is not convenient. Thus, for  $n = 0$

$$F(\lambda) = \lambda + W(\lambda) \equiv \lambda + \frac{(A'\lambda^3 + B'\lambda^2 + C'\lambda + D')k_{se}^{-\tau_s \lambda}}{A\lambda^4 + B\lambda^3 + C\lambda^2 + D\lambda + E} = 0 \quad (A2)$$

Finally, it is shown in reference 3 that, because of the negative exponential in equations (A1) and (A2), the transform in the W-plane of the boundary curve of the right half of the  $\lambda$ -plane degenerates to simply the transform of the imaginary axis. Thus, this curve can be obtained by placing  $i\omega_s$  for  $\lambda$  in equations (A1) and (A2) and letting  $\omega_s$  vary from  $-\infty$  to  $\infty$ . Equations (A1) and (A2) become

$$F(i\omega_s) \equiv 1 + W(i\omega_s) = 0 \quad (A3)$$

for acceleration and velocity autopilots, and

$$F(i\omega_s) \equiv i\omega_s + W(i\omega_s) = 0 \quad (A4)$$

for displacement autopilots.

For displacement autopilots, the critical point in the W-plane corresponding to the origin in the F-plane becomes the point  $-i\omega_s$ , a varying point; that is,  $W(\omega_s)$  must not enclose the point  $(0, -i\omega_s)$ .

## Acceleration Autopilots

The expression for  $W$  as a function of  $\omega_s$  may be obtained for the acceleration autopilot by use of equations (A1) and (A3). For the acceleration autopilot, letting  $a \equiv A'k_s$ ,  $b \equiv B'k_s$ ,  $c \equiv C'k_s$ , and  $d \equiv D'k_s$  gives

$$W(\omega_s) = \frac{[(a\omega_s^4 - c\omega_s^2) + i(d\omega_s - b\omega_s^3)]e^{-i\tau_s\omega_s}}{(A\omega_s^4 - C\omega_s^2 + E) + i(D\omega_s - B\omega_s^3)}$$

or

$$W(\omega_s) = \left[ \frac{(a\omega_s^4 - c\omega_s^2)^2 + (d\omega_s - b\omega_s^3)^2}{(A\omega_s^4 - C\omega_s^2 + E)^2 + (D\omega_s - B\omega_s^3)^2} \right]^{1/2} e^{i(-\omega_s\tau_s + \phi)} \quad (A5)$$

where

$$\phi \equiv \theta_1 - \theta_2 \quad (A6)$$

and

$$\tan \theta_1 = \frac{d\omega_s - b\omega_s^3}{a\omega_s^4 - c\omega_s^2} = \frac{d - b\omega_s^2}{a\omega_s^3 - c\omega_s} \quad (A7a)$$

$$\tan \theta_2 = \frac{D\omega_s - B\omega_s^3}{A\omega_s^4 - C\omega_s^2 + E} \quad (A7b)$$

The angles  $\theta_1$  and  $\theta_2$  may be obtained from these equations for any given value of  $\omega_s$  since the algebraic sign of the numerator of  $\tan \theta$  is the algebraic sign of  $\sin \theta$  and the algebraic sign of the denominator is that of  $\cos \theta$ . These signs determine the proper quadrant for  $\theta$ .

The  $W(\omega_s)$  curve cannot encircle the point  $(-1, 0i)$  in the  $W$ -plane unless  $|W| > 1$ . Thus, the ranges of  $\omega_s$  must be found where  $|W| > 1$  by setting  $|W| = 1$  and solving for  $\omega_s$ . In the following discussion only the part of the curve for positive  $\omega_s$  will be considered inasmuch as the curve for negative  $\omega_s$  is simply the mirror image of the curve for positive  $\omega_s$  in the real axis.

An important result can be obtained by considering what happens to  $W(\omega_s)$  as  $\omega_s \rightarrow \infty$ . The phase angle of  $W$  is seen to spiral around the origin whereas

$$\lim_{\omega_s \rightarrow \infty} |W| = \left| \frac{a}{A} \right| = \left| \frac{k_s K_X^2 C_{n\delta r}}{2\mu_b (K_X^2 K_Z^2 - K_{XZ})} \right| \approx \left| \frac{k_s C_{n\delta r}}{2\mu_b K_Z^2} \right| \quad (A8)$$

Thus,  $W(\omega_s)$  spirals about a circle of this radius, and it can be seen that stability is impossible if the limit is greater than 1, since the point  $(-1, 0i)$  would certainly be enclosed in this case. Therefore, stability is impossible for  $n > 2$  since in this case  $\lim_{\omega_s \rightarrow \infty} |W| = \infty$ .

In the cases of interest the limit of equation (A8) is less than 1. The next step is to find the critical values of  $\omega_s$  by setting  $|W| = 1$ . This condition gives a quartic in  $\omega_s^2$ . If  $x$  is substituted for  $\omega_s^2$ , the critical roots are the positive real roots of the resulting equation

$$(a^2 - A^2)x^4 + (b^2 - B^2 + 2AC - 2ac)x^3 + (c^2 - C^2 + 2BD - 2bd - 2AE)x^2 + (d^2 - D^2 + 2CE)x - E^2 = 0 \quad (A9)$$

When there are no positive real roots of equation (A9), the system is always stable. Moreover, for  $\left| \frac{a}{A} \right| < 1$ , there must always be an even number of such roots (double roots being counted twice). For the one-degree-of-freedom case considered in reference 3 this equation was a quadratic; consequently, there was only one pair of values  $(\omega_{s1}, \omega_{s2})$  for which  $|W| = 1$ , and between these values  $|W| > 1$ . This condition corresponds to the fact that the frequency-response curve of the system has only one maximum. In the three-degree-of-freedom case there are four possible positive real roots, a condition which corresponds to the fact that the frequency-response curve may have two maximums (see fig. 4(a)). Since either of these maximums, in case four critical roots exist, may enclose the point  $(-1, 0i)$ , each pair of successive roots must be treated in the same way as the single pair was treated in reference 3. In most cases equation (A9) will have only two positive real roots. A necessary condition that there be four positive roots is that equation (A9) have four sign changes in its coefficients. The necessary and sufficient conditions for existence of four real roots can be found in most algebra books (for example, reference 7).

Although equation (A9) will usually have only one pair of real positive roots, for the sake of generality the possibility of two pairs must be considered. Corresponding to the two pairs of successive roots  $(\omega_{s1}$  and  $\omega_{s2})$  and  $(\omega_{s1}'$  and  $\omega_{s2}')$ , where  $\omega_{s1}' > \omega_{s2}' > \omega_{s1} > \omega_{s2}$ , two pairs of values  $(\phi_1, \phi_2)$  and  $(\phi_1', \phi_2')$  can be obtained from equations (A6) and (A7). Then, there are two conditions to determine the stable ranges of time lag:

$$\frac{(2m - 1)\pi + \phi_2}{\omega_{s2}} < \tau < \frac{(2m + 1)\pi + \phi_1}{\omega_{s1}} \quad (A10a)$$

$$\frac{(2m - 1)\pi + \phi_2'}{\omega_{s2}'} < \tau < \frac{(2m + 1)\pi + \phi_1'}{\omega_{s1}'} \quad (A10b)$$

For the system to be stable, both of these must be satisfied; that is, the stable time-lag ranges are those where the ranges in equation (A10a) and equation (A10b) overlap. Here  $m = 0, 1, 2, \dots$ . The values of  $m$  for which the stable ranges exist are given by the condition

$$m < \frac{(\pi + \phi_1)\omega_{s2} + (\pi - \phi_2)\omega_{s1}}{2\pi(\omega_{s1} - \omega_{s2})} \quad (A11a)$$

or

$$m < \frac{(\pi + \phi_1')\omega_{s2}' + (\pi - \phi_2')\omega_{s1}'}{2\pi(\omega_{s1}' - \omega_{s2}')} \quad (A11b)$$

Of course the smaller of these two bounding values is actually the largest  $m$  for which stable ranges exist. This value can be used in the corresponding equation (A10a) or (A10b) to find the maximum value of  $\tau$  for stability.

#### Velocity Autopilots

The procedure for velocity autopilots is the same as that for acceleration autopilots, the only difference being that the magnitude of  $W(\omega_s)$  is divided by  $\omega_s$  and the phase angle decreased by  $\pi/2$ . The change in phase angle appears in  $\theta_1$ , which is now given by

$$\tan \theta_1 = \frac{c\omega_s - a\omega_s^3}{d - b\omega_s^2} \quad (A12)$$

Setting  $|W|$  equal to 1 now yields, for  $\omega_s^2 \equiv x$ ,

$$A^2x^4 + (B^2 - a^2 - 2AC)x^3 + (C^2 - b^2 + 2ac + 2AE - 2BD)x^2 + (D^2 - c^2 + 2bd - 2CE)x + E^2 - d^2 = 0 \quad (A13)$$

It might be noted that for this case  $\lim_{\omega_s \rightarrow \infty} |W| = 0$ , so that no condition similar to that of equation (A8) arises. However, in this case,  $|W|$  does not vanish as  $\omega_s \rightarrow 0$ :

$$\lim_{\omega_s \rightarrow 0} |W| = \left| \frac{d}{E} \right| = \left| \frac{2k_s C_{l\beta} C_{n\delta_r}}{C_{n_r} C_{l\beta} - C_{l_r} C_{n\beta} + (C_{l_p} C_{n\beta} - C_{n_p} C_{l\beta}) \tan \gamma} \right| \quad (A14)$$

Since  $|E|$  is generally very small, this quantity will generally be greater than 1. In this case, equation (A13) will have one or three critical roots (usually one), as may be seen from figures 4(b) and 4(c).

In the case  $\left| \frac{d}{E} \right| < 1$  an even number of critical roots will exist, and this case is treated exactly as in the case of the acceleration autopilot by using equations (A10) and the associated discussion, with equation (A12) replacing equation (A7a). However, in the more general case of  $\left| \frac{d}{E} \right| > 1$ , a slightly different treatment is needed.

For the usual case of an odd number of critical values of  $\omega_s$ , the lowest value is treated separately. Call this value  $\omega_{s0}$ . Then,  $|W| > 1$  when  $\omega_s < \omega_{s0}$ , as can be seen in figure 4(b). Since the phase angle  $(-\omega_s \tau + \phi)$  is a monotonically decreasing function of  $\omega_s$  and vanishes in this case for  $\omega_s = 0$ , the first condition for stability becomes  $-\omega_{s0} \tau + \phi_0 > -\pi$ , where  $\phi_0$  is obtained when  $\omega_{s0}$  is used in equations (A12), (A7b), and (A6). Thus, the stability condition for the first maximum of  $|W|$  is the stringent one that

$$\tau < \frac{\pi + \phi_0}{\omega_{s0}} \quad (A15)$$

In the case of one root, this is the only condition. For three roots an additional condition must be satisfied since the second maximum may enclose the point  $(-1, 0i)$ . In this case the remaining two roots, with  $\omega_{s0} < \omega_{s2} < \omega_{s1}$ , are paired just as in the acceleration autopilot, except that equation (A12) of course replaces (A7a), and equation (A10a) applies. Note that both conditions (equations (A10a) and (A15)) must be satisfied for stability, as described in the discussion of the acceleration autopilot.

#### Displacement Autopilots

In comparing equation (A2) with equation (A1) for  $n = 1$ , the  $W(\omega_s)$  in equation (A4) for displacement autopilots can be seen to be exactly the

same as the  $W(\omega_s)$  in equation (A3) for velocity autopilots. The difference between the two cases arises from the change in the critical point of the  $W$ -plane, as pointed out in the paragraph following equation (A4). Only positive values of  $\omega_s$  need be considered, and for these values the critical point is  $(0, -i\omega)$ . Since this point cannot be enclosed except when  $|W| > \omega_s$ , the critical values of  $\omega_s^2$  are given by the positive real roots of  $|W|^2 = \omega_s^2$ , and the critical phase angles are now  $-(2m + \frac{1}{2})\pi$  rather than  $-(2m - 1)\pi$ .

The equation determining the critical values for  $x \equiv \omega_s^2$  is

$$A^2x^5 + (B^2 - 2AC)x^4 + (C^2 - a^2 + 2AE - 2BD)x^3 + (D^2 - b^2 + 2ac - 2CE)x^2 + (E^2 - c^2 + 2bd)x - d^2 = 0 \quad (A16)$$

This equation gives the intersections of the function  $|W|$  with the straight line with unit slope, as shown in figures 4(d) and 4(e). From these figures the equation is seen always to have an odd number of real positive roots (double roots being counted twice); and, in particular, figure 4(e) shows how the maximum of five critical values might occur.

The method of procedure is the same as that given for the velocity autopilots with an odd number of roots. Equations (A12), (A7b), and (A6) are used to get  $\phi(\omega_s)$ . The first critical frequency  $\omega_{s0}$  gives as the stability condition in this case that  $-\omega_{s0}\tau + \phi_0 > -\frac{\pi}{2}$ . Thus, the first stability condition for this case is apparently the very stringent one that

$$\tau < \frac{\frac{\pi}{2} + \phi_0}{\omega_{s0}} \quad (A17)$$

For three critical values, the next two are paired as before and give the additional stability condition for  $\omega_{s0} < \omega_{s2} < \omega_{s1}$ :

$$\frac{(2m - \frac{3}{2})\pi + \phi_2}{\omega_{s2}} < \tau < \frac{(2m + \frac{1}{2})\pi + \phi_1}{\omega_{s1}} \quad (A18)$$

which replaces equation (A10a). Equations (A17) and (A18) must both be satisfied for stability.

Finally, for five critical values, an almost impossible case, the final pair of values  $(\omega_{s2}', \omega_{s1}')$  gives a third necessary condition when used in equation (A18), as described in the discussion of equation (A10b).

## APPENDIX B

DETERMINATION OF MAXIMUM DAMPING OBTAINABLE BY USE  
OF A SPECIFIC AUTOPILOT

The conditions which must be satisfied if the damping curves are to have loops are that  $(\tau_s)_m$  have both a maximum and a minimum value for some values of  $\omega_s$ , say  $(\omega_s)_1$  and  $(\omega_s)_2$ , and that  $(k_s)_m$  be a minimum for some value of  $\omega_s$  which is between  $(\omega_s)_1$  and  $(\omega_s)_2$ . (See fig. 1(d).) The loops will break down when  $\frac{d(k_s)_m}{d\omega_s}$  and  $\frac{d(\tau_s)_m}{d\omega_s}$  vanish for the same value of  $\omega_s$ . The value of  $\omega_s$  for which these conditions are satisfied is the maximum damping of the system obtainable by use of a specific autopilot. A curve representing a damping greater than this maximum in the  $k_s, \tau_s$  plane will have no practical significance, since for every point on this curve some oscillatory mode with less damping than the maximum will always exist.

Now,  $(k_s)_m$  and  $(\tau_s)_m$  are defined by the expressions

$$\left. \begin{aligned} (k_s)_m &= R_2 e^{(\tau_s)_m a} \\ (\tau_s)_m &= \frac{2\pi m - \theta_2}{\omega_s} \end{aligned} \right\} \quad (B1)$$

where  $R_2$ ,  $(\tau_s)_m$ , and  $\theta_2$  are functions of  $\omega_s$  and were discussed in the section entitled "Analysis." Differentiation of equations (B1) results in the expressions

$$\begin{aligned} \frac{d(k_s)_m}{d\omega_s} &= R_2 e^{(\tau_s)_m a} \frac{d}{d\omega_s} [(\tau_s)_m a] + e^{(\tau_s)_m a} \frac{dR_2}{d\omega_s} \\ \frac{d(\tau_s)_m}{d\omega_s} &= \frac{-\omega_s \frac{d\theta_2}{d\omega_s} - 2\pi m + \theta_2}{\omega_s^2} \end{aligned}$$

Setting these expressions equal to zero and considering  $m = 1$  gives



$$\left. \begin{aligned} \frac{dk_s}{d\omega_s} &= aR_2 \frac{d\tau_s}{d\omega_s} + \frac{dR_2}{d\omega_s} = 0 \\ \frac{d\tau_s}{d\omega_s} &= 2\pi - \theta_2 + \omega_s \frac{d\theta_2}{d\omega_s} = 0 \end{aligned} \right\} \quad (B2)$$

Since  $\frac{d\tau_s}{d\omega_s} = 0$  is a necessary condition,  $\frac{dR_2}{d\omega_s}$  must also be equal to zero if  $\frac{dk_s}{d\omega_s}$  is to vanish. The expressions for  $R_2$  and  $\theta_2$  are both functions of  $\omega_s$ , with the quantity  $a$  as a parameter. Equations (B2) should therefore be solved simultaneously in order to determine the maximum obtainable damping since

$$T_{1/2} = \frac{-0.693}{a} \frac{b}{V}$$

A convenient method for determining the maximum obtainable damping is as follows: For several values of  $a$  for which the loops are known to be small, determine the values of  $\omega_s$  for which  $\frac{dR_2}{d\omega_s} = 0$ . Substitute these combinations of  $a$  and  $\omega_s$  into the expression  $\frac{d\tau_s}{d\omega_s}$  and evaluate the function. A plot may then be made of  $\frac{d\tau_s}{d\omega_s}$  against  $a$  as abscissa, and the value of  $a$  for which  $\frac{d\tau_s}{d\omega_s} = 0$  is the required solution. As a check, this value of  $a$  should be substituted into  $\frac{dR_2}{d\omega_s} = 0$  and the corresponding value of  $\omega_s$  determined. This combination of  $a$  and  $\omega_s$ , if a solution, will then satisfy  $\frac{d\tau_s}{d\omega_s} = 0$ .

The same analysis is applicable to the loops corresponding to  $m = 2, 3, \dots$ . Equations (B1) show that  $R_2$  and  $\theta_2$  are independent of  $m$ ; hence,  $\frac{dR_2}{d\omega_s}$  is also independent of  $m$ . The general expression for  $\frac{d(\tau_s)_m}{d\omega_s} = 0$  is (see equations (B2))

$$2\pi m - \theta_2 + \omega_s \frac{d\theta_2}{d\omega_s} = 0$$

Rearranging the equation gives

$$2\pi m = \theta_2 - \omega_s \frac{d\theta_2}{d\omega_s} \quad (B3)$$

Thus, if the combinations of  $a$  and  $\omega_s$  which satisfy  $\frac{dR_2}{d\omega_s}$  are determined for a sufficiently wide range of  $a$  and substituted into the right-hand side of equation (B3), the value of  $a$  for which loops will cease to exist for any value of  $m$  can be determined. For example, the  $m = 1$  loops will break down when  $\theta_2 - \omega_s \frac{d\theta_2}{d\omega_s} = 2\pi$ ; the  $m = 2$  loops, when this expression equals  $4\pi$ ; and so on. In general, the value of  $a$  for which the loops break down decreases as  $m$  increases.

The preceding analysis was applied to the  $m = 2$  and  $m = 3$  case for  $T_{1/2} = 0.70$  second since these loops were known to have broken down for this damping (see fig. 1(e)). As was expected, the analysis verified the fact that the loops did not exist for these values of  $m$  for  $T_{1/2} = 0.70$  second.

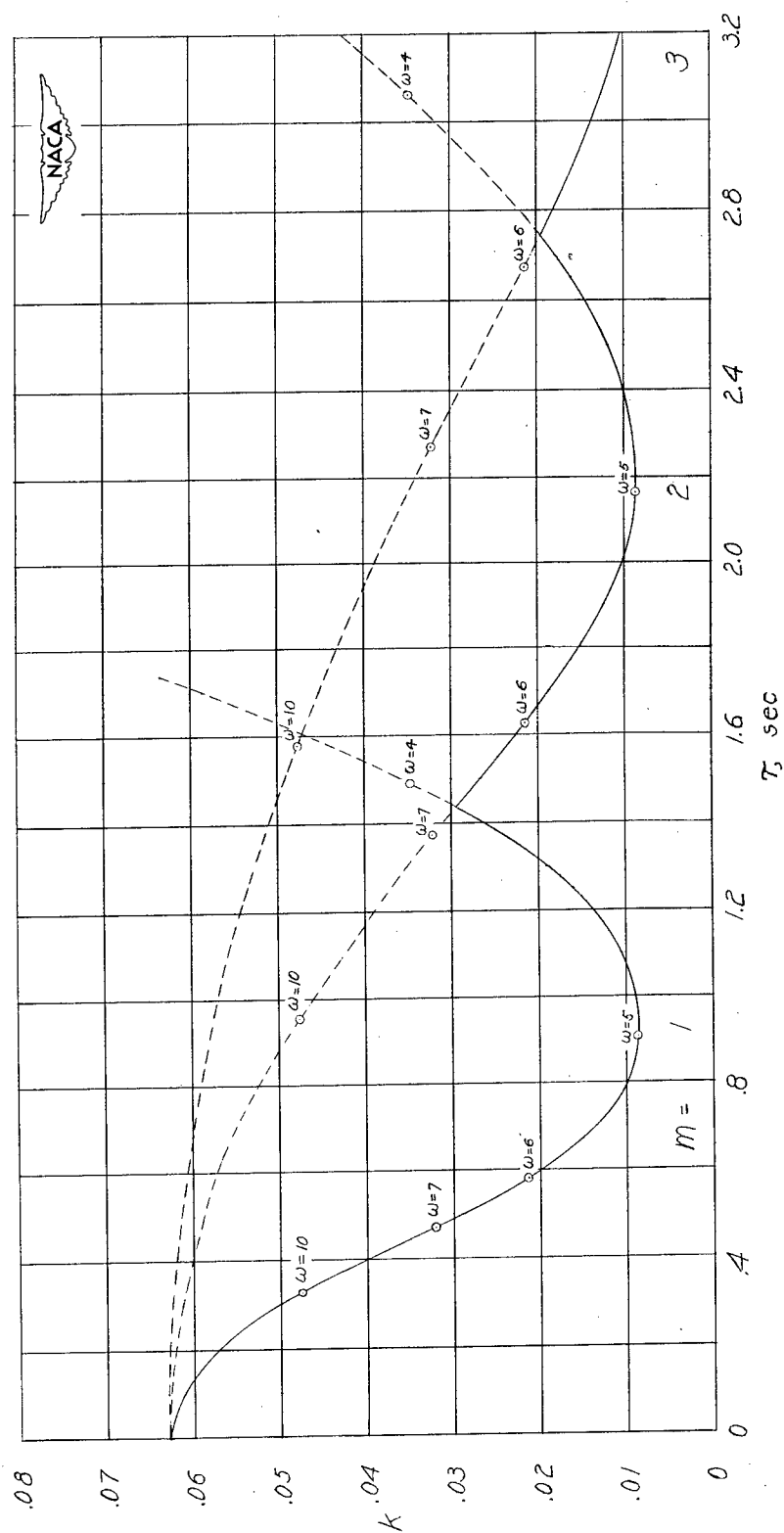
## REFERENCES

1. Greenberg, Harry: Frequency-Response Method for Determination of Dynamic Stability Characteristics of Airplanes with Automatic Controls. NACA Rep. 882, 1947.
2. Brown, Gordon S., and Campbell, Donald P.: Principles of Servomechanisms. John Wiley & Sons, Inc., 1948, pp. 170-174.
3. Ansoff, H. I.: Stability of Linear Oscillating Systems with Constant Time Lag. Jour. Appl. Mech., vol. 16, no. 2, June 1949, pp. 158-164.
4. Sternfield, Leonard, and Gates, Ordway B., Jr.: A Theoretical Analysis of the Effect of Time Lag in an Automatic Stabilization System on the Lateral Oscillatory Stability of an Airplane. NACA TN 2005, 1950.
5. Sternfield, Leonard: Effect of Automatic Stabilization on the Lateral Oscillatory Stability of a Hypothetical Airplane at Supersonic Speeds. NACA TN 1818, 1949.
6. Hurwitz, Adolf, and Courant, R.: Allgemeine Funktionentheorie und elliptische Funktionen, and Geometrische Funktionentheorie. Bd. III of Mathematischen Wissenschaften. Julius Springer (Berlin), 1929, pp. 104-107.
7. Dickson, Leonard Eugene: Elementary Theory of Equations. John Wiley & Sons, Inc., 1917.

TABLE I  
MASS CHARACTERISTICS AND STABILITY DERIVATIVES OF A  
TYPICAL PRESENT-DAY AIRPLANE

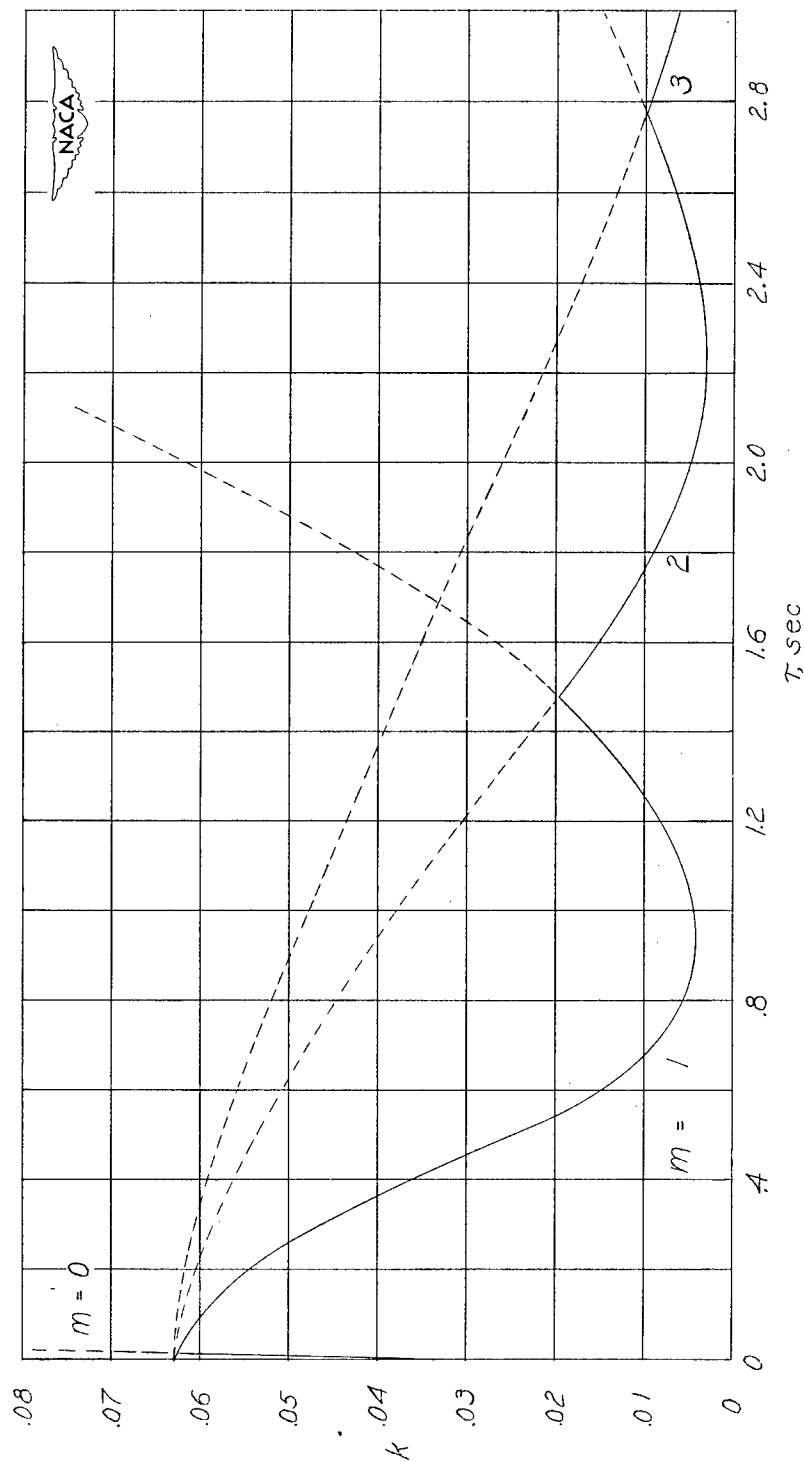
W/S, lb/sq ft . . . . .	65
S, sq ft . . . . .	130
b, ft . . . . .	28
$\rho$ , slugs/cu ft . . . . .	0.00089
V, ft/sec . . . . .	797
$\gamma$ , deg . . . . .	0
CL . . . . .	0.23
$\mu_b$ . . . . .	80.7
$K_X^2$ . . . . .	0.00967
$K_Z^2$ . . . . .	0.0513
$K_{XZ}$ . . . . .	-0.00145
$\eta$ , deg . . . . .	-2.0
$C_{l_p}$ , per radian . . . . .	-0.40
$C_{l_r}$ , per radian . . . . .	0.08
$C_{n_p}$ , per radian . . . . .	-0.016
$C_{n_r}$ , per radian . . . . .	-0.40
$C_{Y_p}$ , per radian . . . . .	0
$C_{Y_r}$ , per radian . . . . .	0
$C_{Y_\beta}$ , per radian . . . . .	-1.0
$C_{n_\beta}$ , per radian . . . . .	0.25
$C_{l_\beta}$ , per radian . . . . .	-0.13
$C_{n_{\delta_r}}$ , per radian . . . . .	-0.163





(a)  $T_1/2 = \infty$ .

Figure 1.- Curves of constant damping of the lateral oscillations of the airplane described in table I equipped with an autopilot sensitive to yawing acceleration.



(b)  $T_1/2 = 3.50$ .

Figure 1.- Continued.

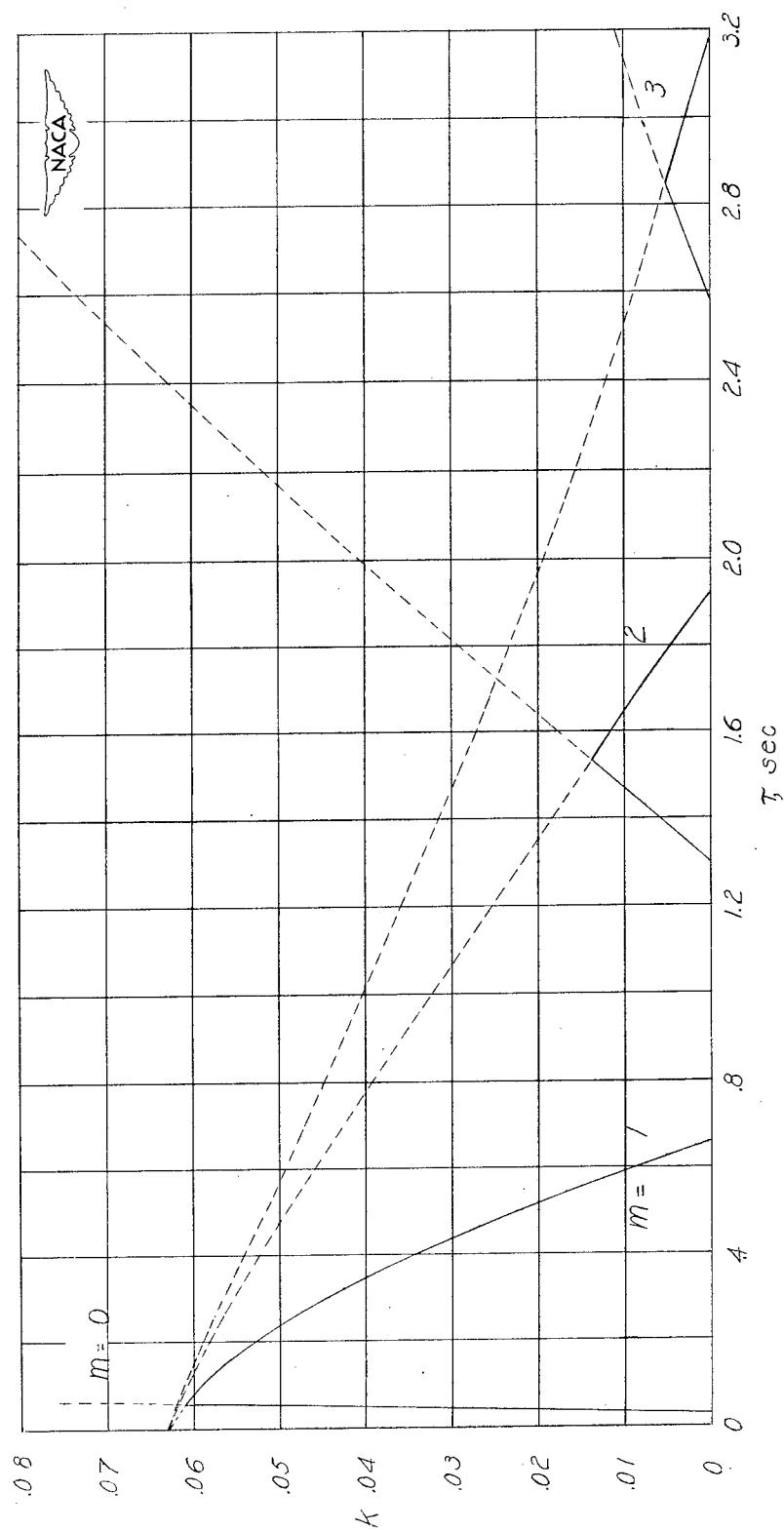
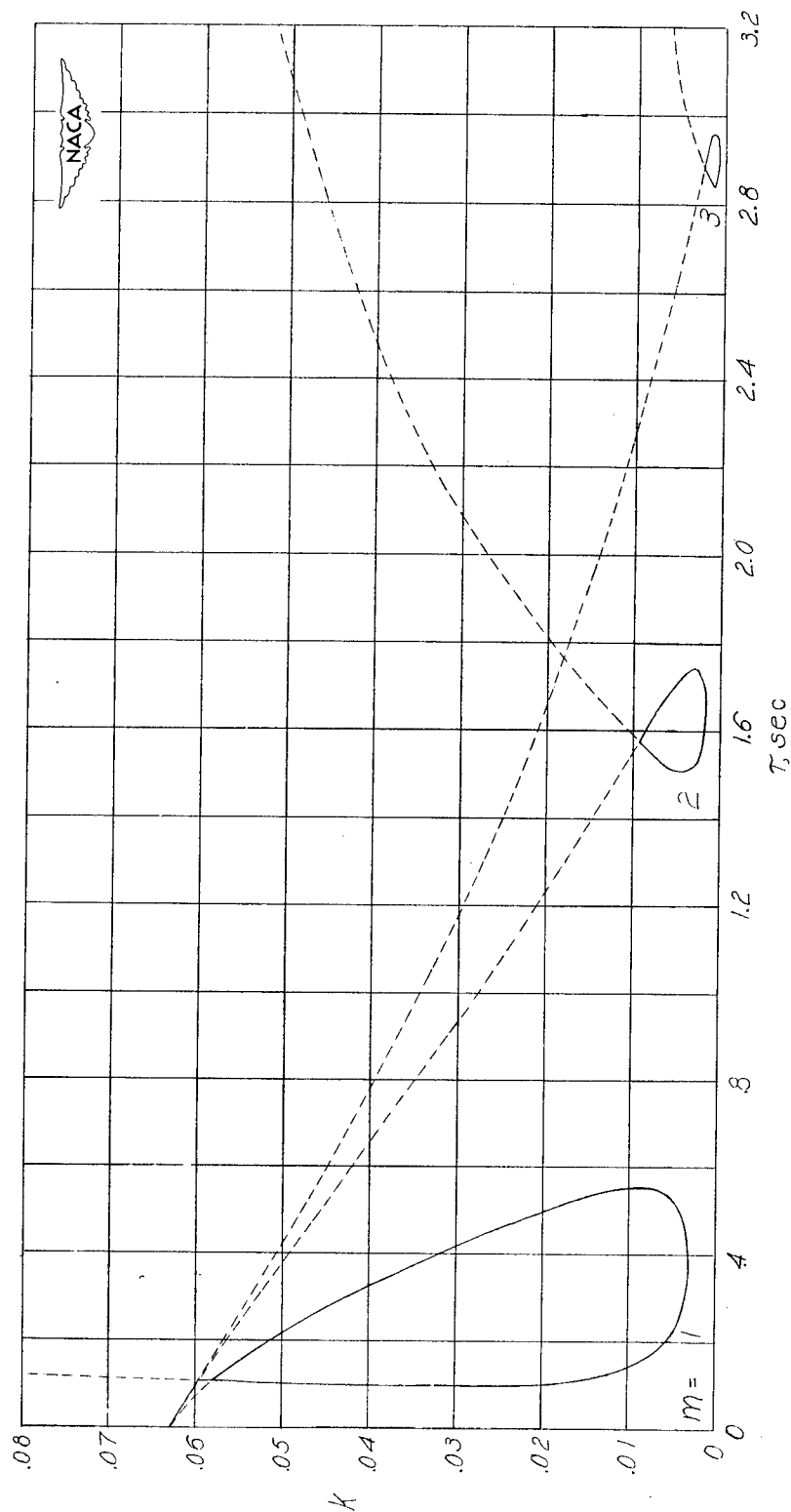
(c)  $T_1/2 = 2.02$ .

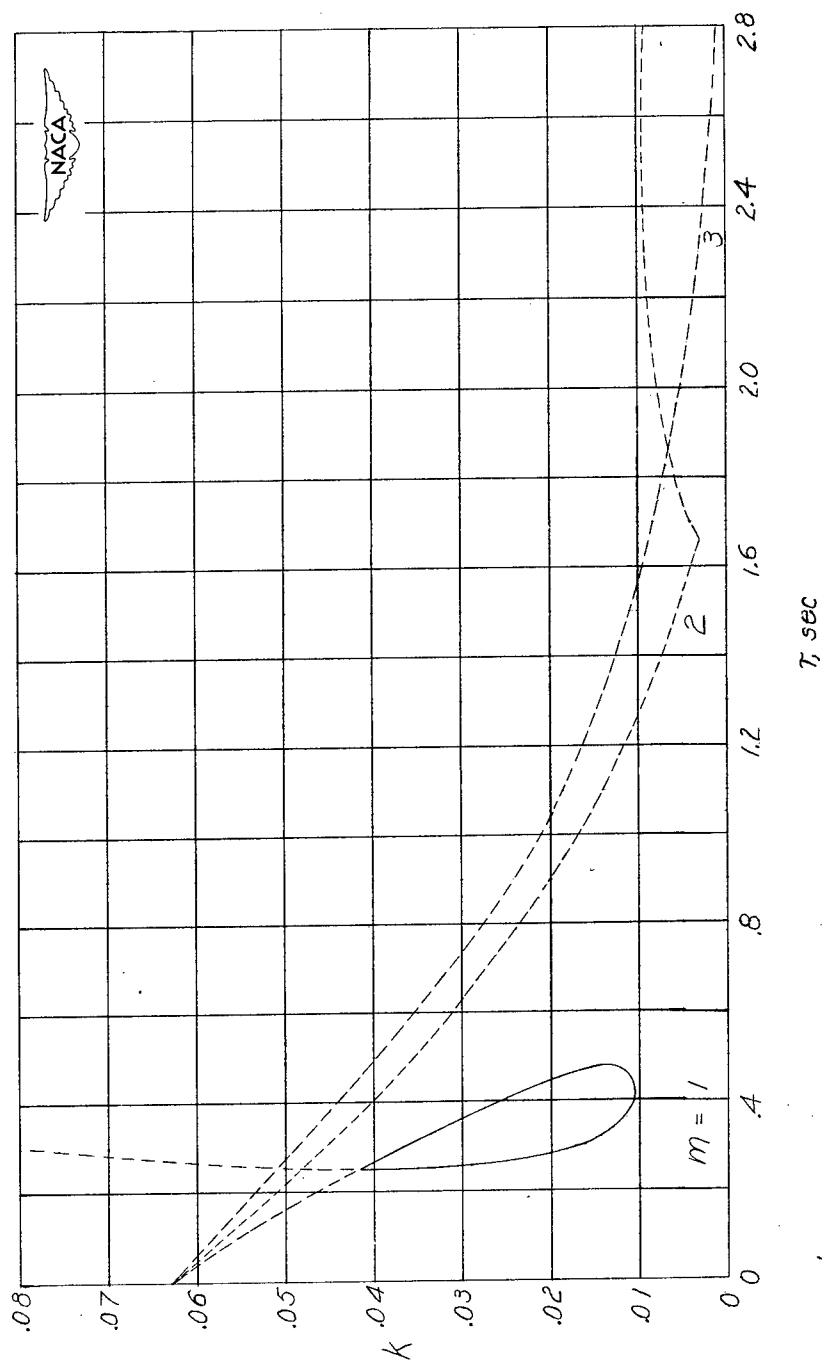
Figure 1.- Continued.



(a)  $T_L/2 = 1.40$ .

Figure 1.- Continued.





(e)  $T_1/2 = 0.70$ .

Figure 1.- Concluded.

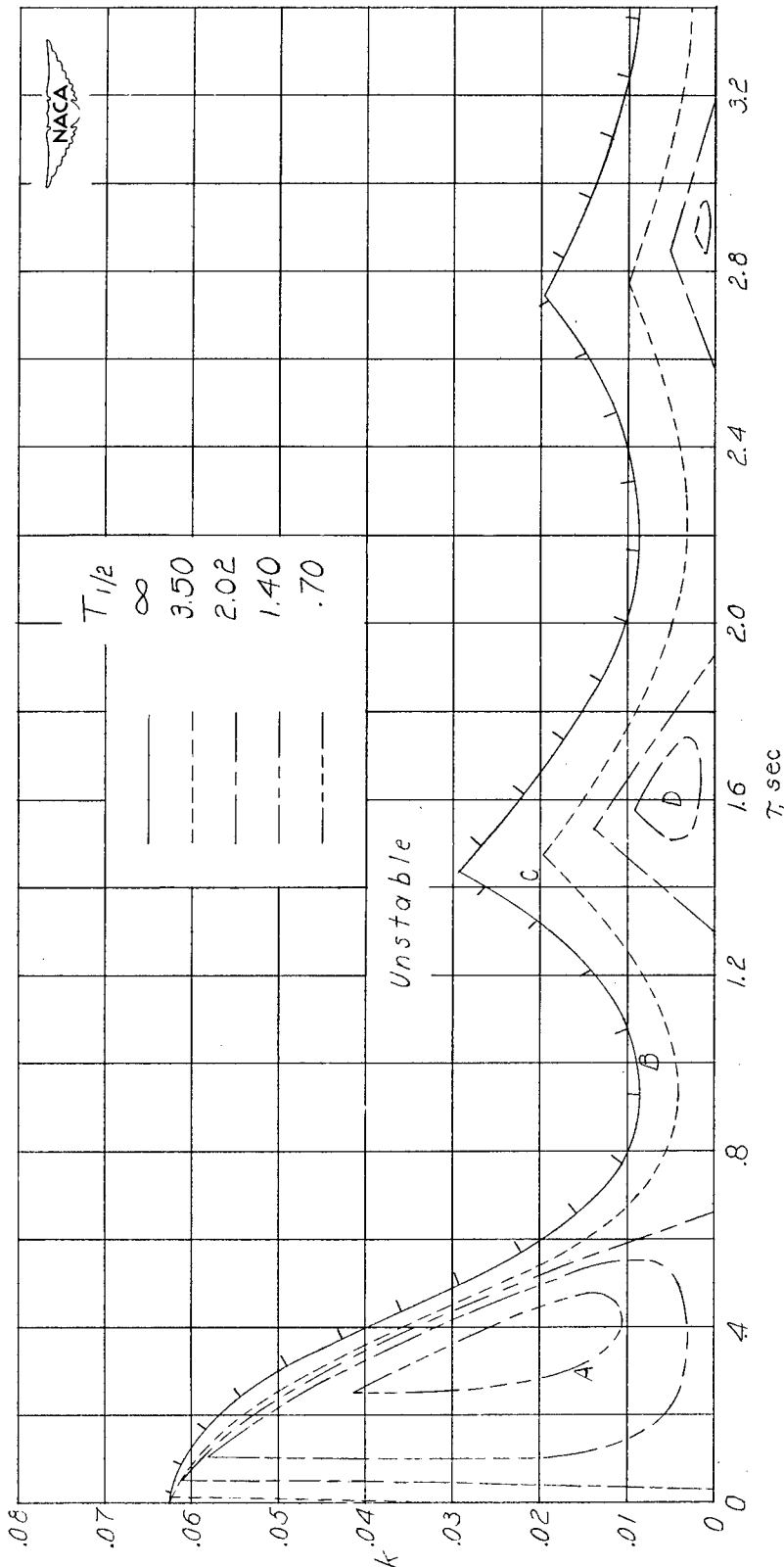
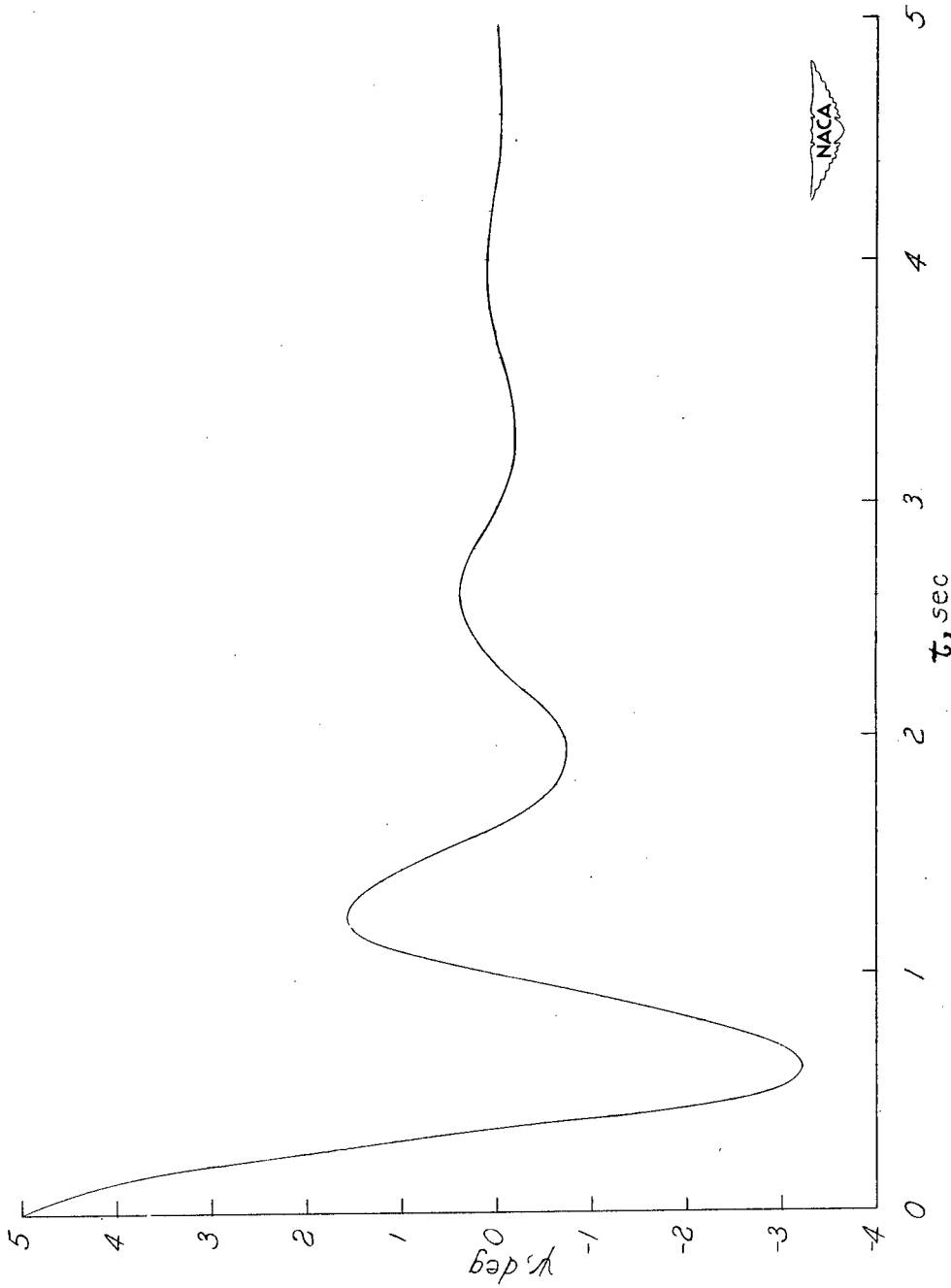
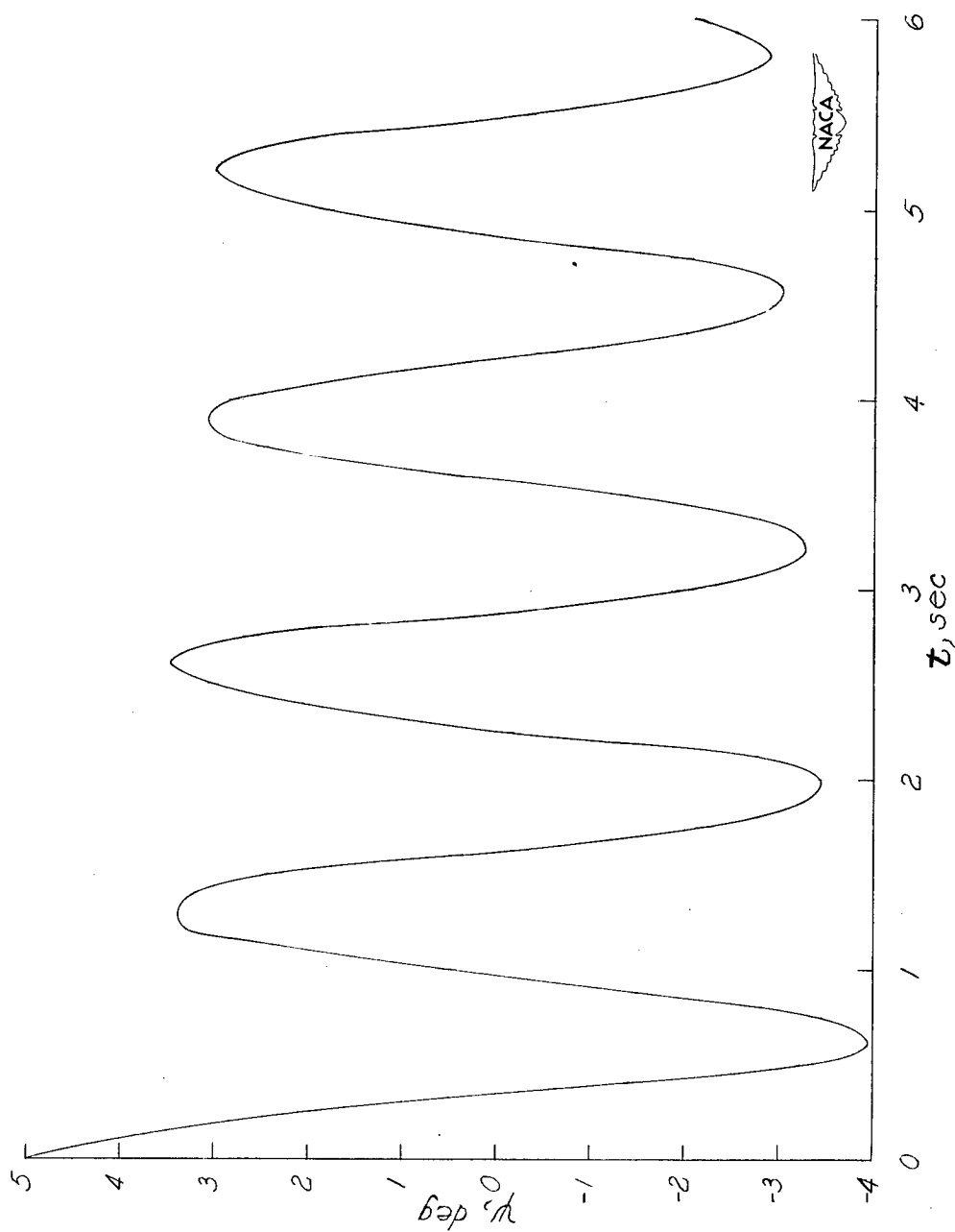


Figure 2.- Ranges of  $k$  and  $\tau$  required for various amounts of damping of the lateral oscillations of the airplane-autopilot system obtained from figure 1.



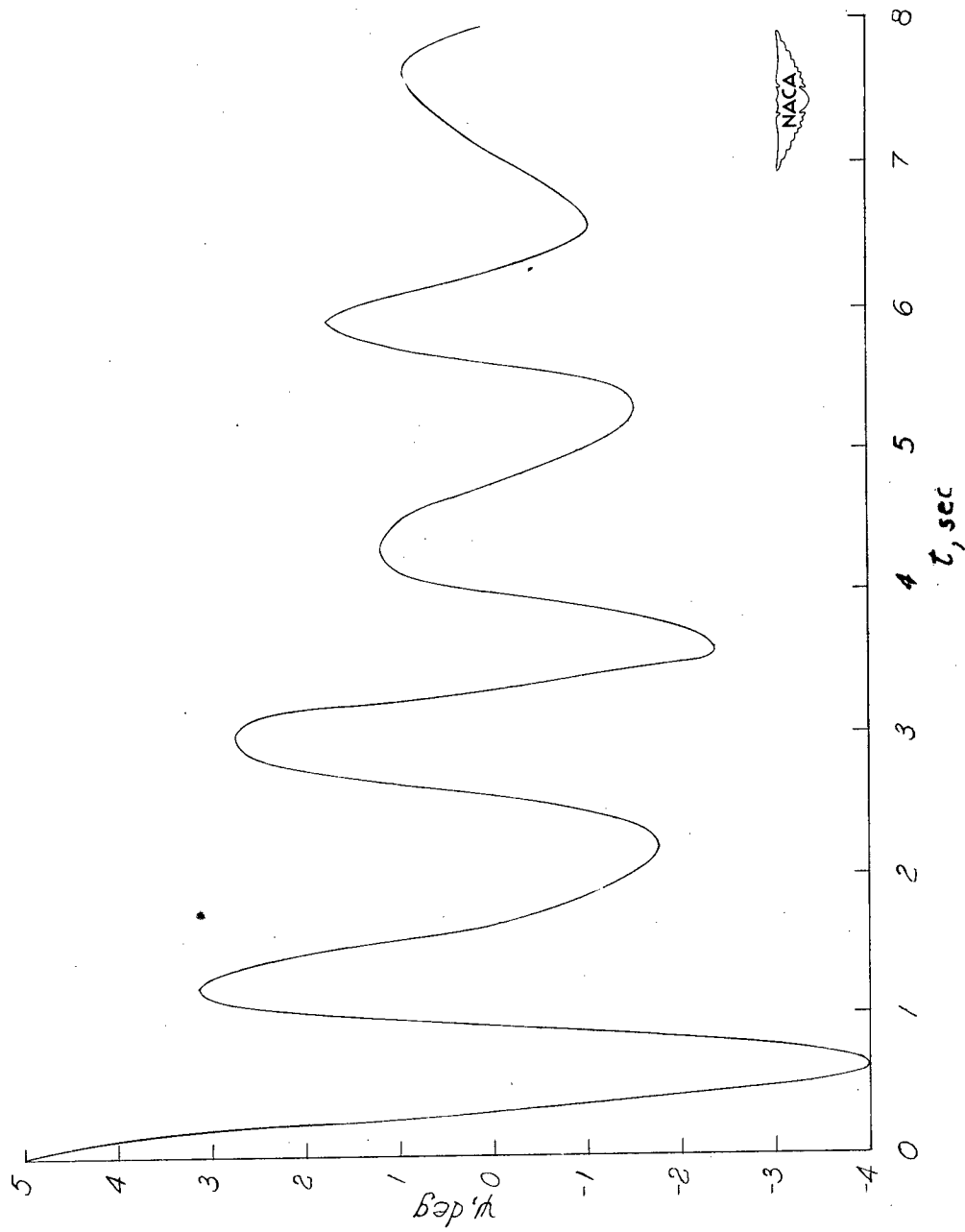
(a)  $\tau = 0.30$ ;  $k = 0.015$  (point A, fig. 2).

Figure 3.- Airplane motion in yaw subsequent to an initial displacement in yaw for several combinations of  $k$  and  $\tau$ .



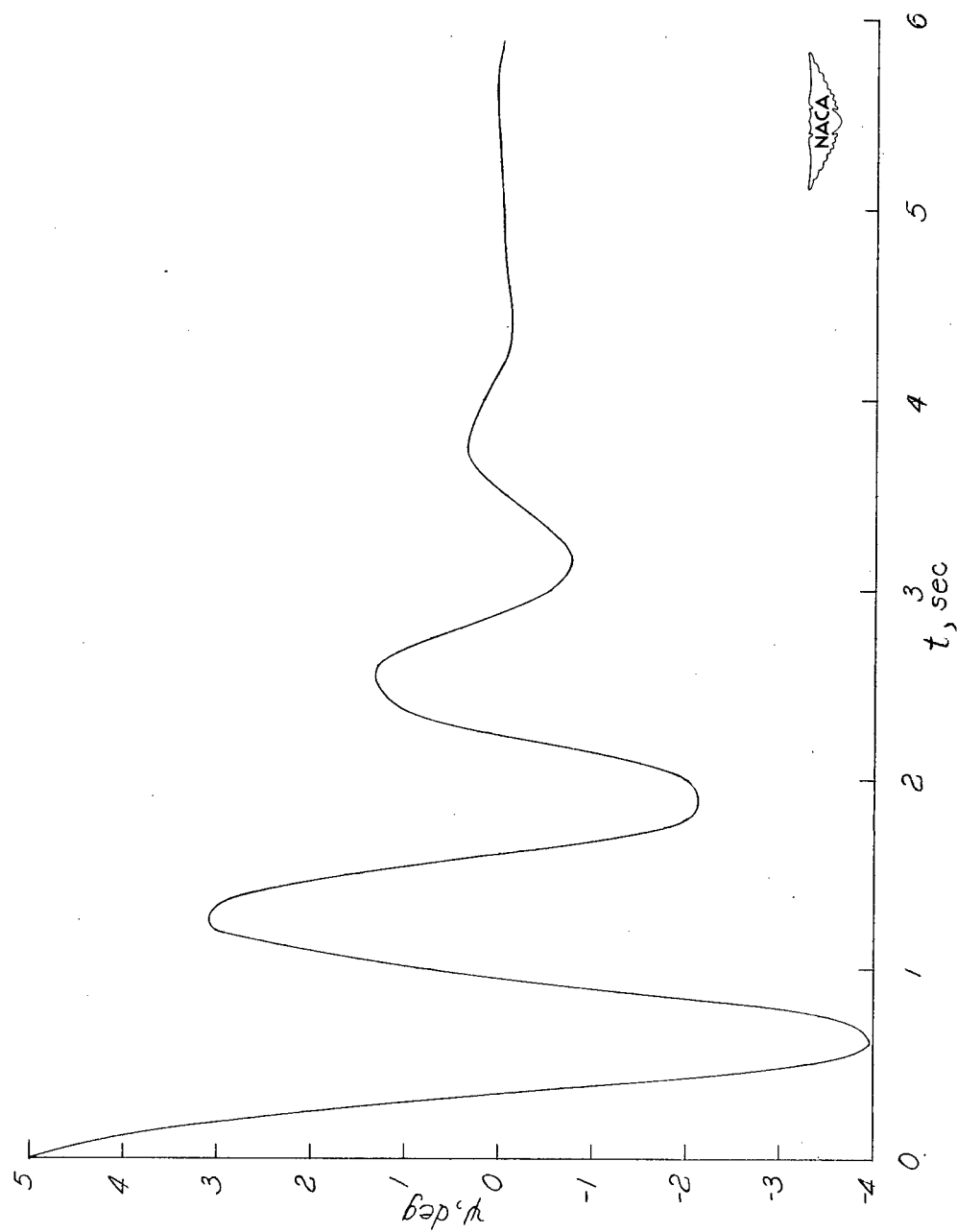
(b)  $\tau = 1.0$ ;  $k = 0.0075$  (point B, fig. 2).

Figure 3.- Continued.



(c)  $\dot{\tau} = 1.43$ ;  $k = 0.0215$  (point C, fig. 2).

Figure 3.- Continued.



(d)  $\tau = 1.6$ ;  $k = 0.005$  (point D, fig. 2).

Figure 3.- Concluded.

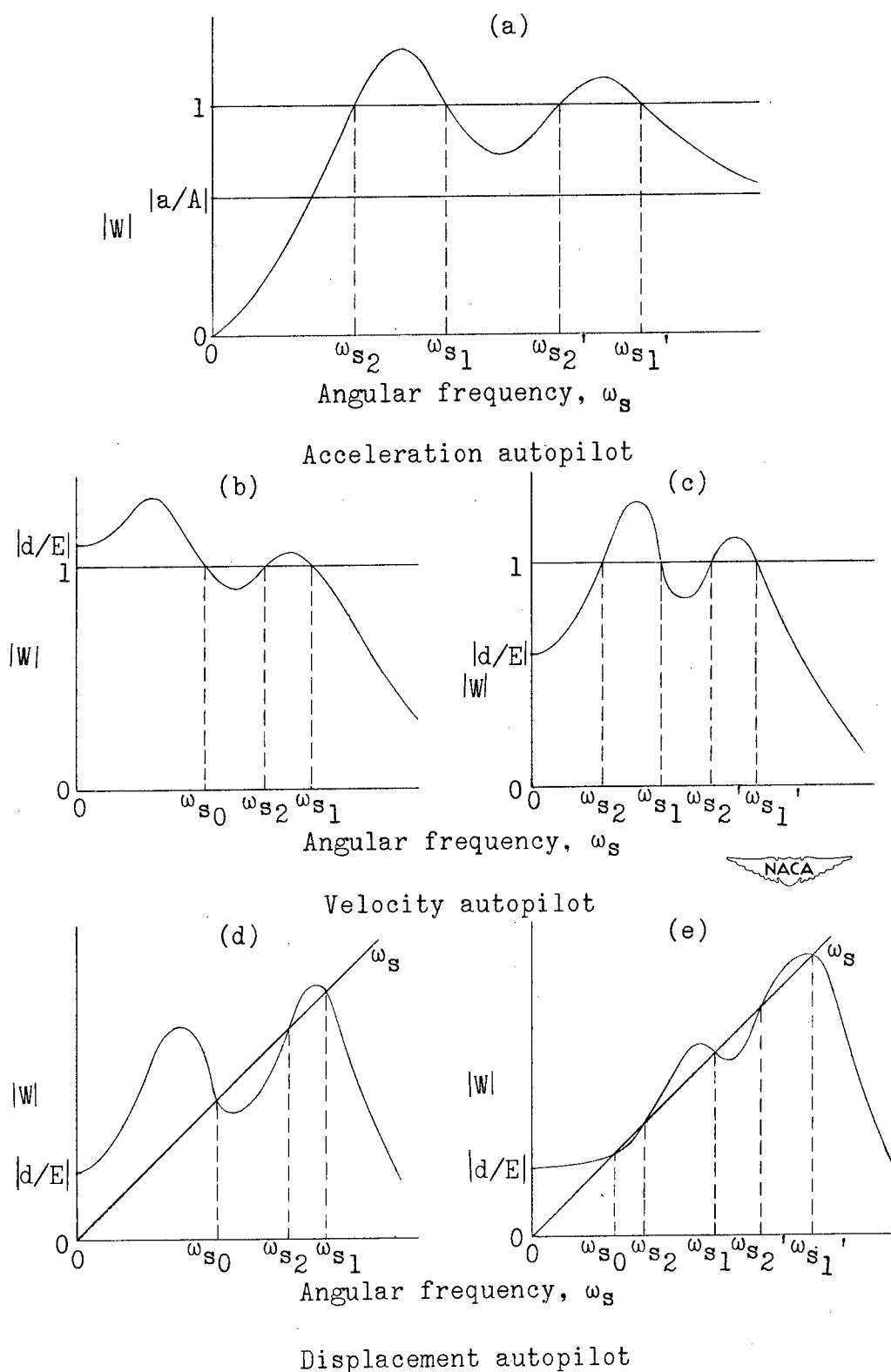


Figure 4.- Types of frequency response for  $|W|$  showing possible critical frequencies for acceleration, velocity, and displacement yaw autopilots.

Stability, Lateral and  
Directional - Dynamic

1.8.1.2.2



A Theoretical Method of Determining the Control Gearing and Time Lag Necessary for a Specified Damping of an Aircraft Equipped with a Constant-Time-Lag Autopilot.

By Ordway B. Gates, Jr., and Albert A. Schy

NACA TN 2307

March 1951

(Abstract on Reverse Side)

Stabilization, Automatic

1.8.8



A Theoretical Method of Determining the Control Gearing and Time Lag Necessary for a Specified Damping of an Aircraft Equipped with a Constant-Time-Lag Autopilot.

By Ordway B. Gates, Jr., and Albert A. Schy

NACA TN 2307

March 1951

(Abstract on Reverse Side)